Title: Dissecting unique and common variance across body and brain health indicators using age prediction

Authors: Dani Beck[1,2,3], Ann-Marie G. de Lange[3,4,5], Tiril P. Gurholt[1], Irene Voldsbekk[1,3], Sivaniya Subramaniapillai[3,4], Louise Schindler[3,4], Guy Hindley[1], Esten H. Leonardsen[1,3], Zillur Rahman[1], Dennis van der Meer[1,6], Max Korbmacher[1, 7] Jennifer Linge[8,9], Olof D. Leinhard[8,9], Karl T. Kalleberg[10], Andreas Engvig[11], Ida Sønderby[1,12,13], Ole A. Andreassen[1,13], Lars T. Westlye[1,3,13]

[1] NORMENT, Division of Mental Health and Addiction, Oslo University Hospital & Institute of Clinical Medicine, University of Oslo, Norway

[2] Department of Psychiatric Research, Diakonhjemmet Hospital, Oslo, Norway

[3] Department of Psychology, University of Oslo, Norway

[4] LREN, Centre for Research in Neurosciences-Department of Clinical Neurosciences, CHUV and University of Lausanne, Lausanne, Switzerland

[5] Department of Psychiatry, University of Oxford, Oxford, United Kingdom

[6] School of Mental Health and Neuroscience, Faculty of Health, Medicine and Life Sciences, Maastricht University, Maastricht, The Netherlands

[7] Department of Health and Functioning, Western Norway University of Applied Sciences, Bergen, Norway

[8] AMRA Medical AB, Linköping, Sweden

[9] Division of Diagnostics and Specialist Medicine, Department of Health, Medicine and Caring Sciences, Linköping University, Linköping, Sweden

[10] Age Labs AS, Oslo, Norway

[11] Department of Endocrinology, Obesity and Preventive Medicine, Section of Preventive Cardiology, Oslo University Hospital, Oslo, Norway

[12] Department of Medical Genetics, Oslo University Hospital, Oslo, Norway

[13] KG Jebsen Centre for Neurodevelopmental Disorders, University of Oslo

* Corresponding author: Dani Beck (dani.beck@psykologi.uio.no)

Abstract

Ageing is a heterogeneous multisystem process involving different rates of decline in physiological integrity across biological systems. The current study dissects the unique and common variance across body and brain health indicators and parses inter-individual heterogeneity in the multisystem ageing process. Using machine-learning regression models on the UK Biobank dataset (N = 32,593, age range 44.6-82.3, mean age 64.1 years), we first estimated tissue-specific brain age for white and gray matter based on diffusion and T1-weighted magnetic resonance imaging (MRI) data respectively. Next, bodily health traits including cardiometabolic, anthropometric and body composition measures of adipose and muscle tissue from bioimpedance and body MRI were combined with brain MRI data to predict age for a body-brain age model. The results showed that the models including bodily health traits showed significantly higher age prediction accuracy than models trained solely on brain MRI data. Bayesian multilevel modelling carried out to quantify the associations between health traits and predicted age discrepancies showed that relative to the predictions based only on brain MRI, higher systolic blood pressure and muscle-fat infiltration levels contributed to an increase in predicted age, suggesting a link between poor health markers and older-apparent physiological age. In contrast, higher muscle volume and hand-grip strength contributed to a decrease in predicted age. While these findings corroborate the common notion of a close connection between somatic and brain health, the use of age prediction models allows for an individual-level dissection of the health-related factors that affect the estimated age of an individual. In conclusion, the results suggest that bodily health traits, together with brain imaging features, can provide a more comprehensive and individualised understanding of the ageing processes.

Key words: Ageing, cardiometabolic, brain age, health, body composition

1. Introduction

Ageing has been defined as a multisystem and time-dependent process involving progressive loss of functional and physiological integrity (López-Otín et al., 2013). While advanced age is a primary risk factor for cardiovascular and neurodegenerative diseases, ageing is highly heterogeneous, with differential ageing rates across biological systems and individuals (Cevenini et al., 2008). This has motivated a wealth of research into better understanding the determinants of individual differences in ageing and its relevance to diverse disease processes.

Several biomarkers of normal ageing including body composition and health traits have been proposed (Cole et al., 2019). Changes in blood lipids, adipose and muscle tissue distribution, blood pressure, heart rate, hand grip strength, and anthropometric measures such as body mass index (BMI) and waist-to-hip ratio (WHR) are all associated with ageing (Massy-Westropp et al., 2011; Mielke et al., 2010; Rodgers et al., 2019; Sebastiani et al., 2017). Despite these measures being classified as markers of normal body function rather than disease-specific biomarkers, recent studies have highlighted their utility for risk detection and disease monitoring across cardiovascular disease and dementia (Brain et al., 2023). For example, research has suggested that dysregulation in lipid metabolism in Alzheimer's disease may predict cognitive decline (Wong et al., 2017).

Age prediction using machine learning applied to brain magnetic resonance imaging (MRI) data has enabled individual-level age prediction with high accuracy based on brain white (WM) and gray matter (GM) characteristics derived from diffusion and T1-weighted MRI scans (Beck et al., 2021; Cole et al., 2017; Leonardsen et al., 2022), providing neuroanatomical markers of brain health and integrity (Cole & Franke, 2017; Franke et al., 2010). Although bodily health traits have demonstrated their influence on brain ageing (Beck, de Lange, Alnæs, et al., 2022; Beck, de Lange, Pedersen, et al., 2022; de Lange et al., 2020; Franke et al., 2013, 2014; Kolenic et al., 2018; Ronan et al., 2016), rates of brain and body ageing processes may be partly distinct at the individual level.

Recent work demonstrated the relevance of age prediction based on various organ structures (Tian et al., 2023), reporting that body- and brain-specific age estimates can be differentially influenced by lifestyle and environmental factors. However, the degree to which bodily health traits used in combination with brain imaging features improves age prediction has to our knowledge not been investigated. Combining these features in one model may help distinguish the unique and common variance across indicators of body and

brain health, and parse inter-individual heterogeneity in the multisystem ageing process. Further, this approach contributes to identifying key health traits that influence age predictions beyond the variance captured by the brain measures.

The current study utilised the UK Biobank sample (N = 32,593, mean age = 64.1, SD = 7.5) to assess differences in individual age predictions when adding a variety of body composition and health traits to brain age models based on diffusion- and T1-weighted brain MRI measures. Bodily health traits included cardiometabolic factors, anthropometric measures, and body composition measures of adipose and muscle tissue from bioimpedance and body MRI. Based on the documented connections between brain and body health, we anticipated that models including both bodily health traits and brain MRI features would to a large extent resemble those trained solely on brain MRI data, but with increased age prediction accuracy due to unique variance explained by the bodily health traits. Further, we expected to observe individual variation in the difference between predictions, i.e., a variation in body-brain and brain age predictions across individuals. Lastly, we assessed the extent to which specific markers of bodily health, such as blood pressure, abdominal adiposity, and muscle volume, contributed to differences in individual age predictions.

2. Methodology

2.1. Population

The sample was drawn from the UK Biobank (UKB) (http://www.ukbiobank.ac.uk). All participants provided signed informed consent. UKB has IRB approval from Northwest Multi-centre Research Ethics Committee and its Ethics Advisory Committee (https://www.ukbiobank.ac.uk/ethics) oversees the UKB Ethics & Governance Framework (Miller et al., 2016). Specific details regarding recruitment and data collection procedures have been previously published (Collins, 2007). The present study uses the UKB Resource under Application Number 27412. Exclusion criteria included disorders that affect the brain based on ICD10 diagnoses and those with a self-reported long-standing illness disability, diabetes, stroke history.

To remove poor-quality T1-weighted brain MRI data, participants with Euler numbers (Rosen et al., 2018) ± 4 standard deviations from the mean were excluded. For diffusion-weighted (dMRI) data, quality control was assured using the YTTRIUM algorithm (Maximov et al., 2021). A total of N = 160 participants were removed for T1 and dMRI data. Body MRI measurements were quality checked by two independent, trained operators

visually inspecting the images prior to upload to UKB and this has been followed by control of all outliers for anatomical correctness.

For health traits (hereby used as an umbrella term including all body composition and health markers, outliers (values ± 5 SD from the mean) were excluded (N = 627) from the analysis by converting the values to NA, thereby keeping the participant in the sample with their respective non-outlier data. SI Figures 1 and 2 show distributions of health traits before and after quality control. SI Figure 3 shows the prevalence of NA/missing data in the final sample. Following cleaning, the final sample consisted of 32,593 individuals (Females: N = 17,200, mean age = 63.6, SD = 7.37, Males: N = 15,393, mean age = 64.71, SD = 7.63) with T1, dMRI, and body health trait data. Table 1 summarises the health trait descriptive statistics.

2.2. MRI data acquisition and processing

A detailed overview of the full UKB data acquisition and image processing protocol is available in Alfaro et al. (2018) and Miller et al. (2016). Briefly, brain MRI data were acquired on a 3 Tesla Siemens 32-channel Skyra scanner. T1-weighted MPRAGE and T2-weighted FLAIR volumes were both acquired in sagittal orientation at 1x1x1 mm. Processing protocols followed a harmonised analysis pipeline, including automated surface-based morphometry and subcortical segmentation using FreeSurfer version 5.3 (Fischl et al., 2002). A standard set of subcortical and cortical summary statistics were used from FreeSurfer (Fischl et al., 2002), as well as a fine-grained cortical parcellation scheme (Glasser et al., 2016) to extract GM cortical thickness, cortical surface area, and volume for 180 regions of interest per hemisphere. This yielded a total set of 1,118 structural brain imaging features (360/360/360/38 for cortical thickness/area/volume, as well as cerebellar/subcortical and cortical summary statistics, respectively) that were used as input features in the GM-specific age prediction model in line with recent implementations (de Lange et al., 2019; Kaufmann et al., 2019; Schindler et al., 2022).

For dMRI, a conventional Stejskal-Tanner monopolar spin-echo echo-planar imaging sequence was used with multiband factor 3. Diffusion weightings were 1,000 and 2,000 s/mm^2 and 50 non-coplanar diffusion directions per each diffusion shell. The spatial resolution was 2□mm^3 isotropic, and five anterior-posterior versus three anterior-posterior images with b =□0 s/mm^2 were acquired. Data were processed using a previously described pipeline (Maximov et al., 2019). Metrics derived from diffusion tensor imaging (DTI) (Basser, 1995), diffusion kurtosis imaging (DKI) (Jensen et al., 2005), WM tract integrity

(WMTI) (Fieremans et al., 2011), and spherical mean technique (SMT) (Kaden et al., 2016) were used as input features in the WM-specific age prediction model, as described in Voldsbekk et al. (2021). Tract-based spatial statistics (TBSS) was used to extract diffusion metrics in WM (Smith et al., 2006) (see Voldsbekk et al. (2021) for full pipeline). For each metric, WM features were extracted based on John Hopkins University (JHU) atlases for WM tracts and labels (with 0 thresholding) (Mori et al., 2006), including global mean values and regional measures (Beck et al., 2021; Subramaniapillai et al., 2022; Voldsbekk et al., 2021). The diffusion MRI data passed TBSS post-processing quality control using the YTTRIUM algorithm (Maximov et al., 2020), and were residualised with respect to scanning site using linear models.

The methods used to generate the body MRI-derived measurements have been described and evaluated in more detail elsewhere (Borga et al., 2018, 2020; Karlsson et al., 2015; Linge et al., 2018; West et al., 2018). Briefly, the process for fat and muscle compartments includes the following steps: (1) calibration of fat images using fat-referenced MRI, (2) registration of atlases with ground truth labels for fat and muscle compartments to the acquired MRI dataset to produce automatic segmentation, (3) quality control by two independent trained operators including the possibility to adjust and approve the final segmentation, and (4) quantification of fat volumes, muscle volumes and muscle-fat infiltration within the segmented regions. For liver proton density fat fraction (PDFF), nine regions of interest (ROI) were manually placed, evenly distributed in the liver volume, while avoiding major vessels and bile ducts.

2.3. Body composition and health traits

Table 1 summarises the descriptive statistics of the health traits used in the study. A detailed description of each variable can be found in Supplementary Information (SI) Section 1.

Table 1. Descriptive statistics pertaining to each health trait, including mean ± standard deviation (SD).

Health trait	Abbreviation	Full sample (N = 32,593)	Female (N = 17,200)	Male (N = 15,393)
Adipose and muscle tissue from body MRI				
Visceral adipose tissue, *L*	VAT	3.62 ± 2.20	2.58 ± 1.48	4.78 ± 2.27
Abdominal subcutaneous adipose tissue, *L*	ASAT	6.81 ± 3.10	7.79 ± 3.30	5.72 ± 2.42
Anterior thigh muscle volume, *L*	ATMV	1.70 ± 0.48	1.34 ± 0.23	2.11 ± 0.35
Posterior thigh muscle volume, *L*	PTMV	3.36 ± 0.80	2.75 ± 0.38	4.10 ± 0.55

Anterior thigh muscle-fat infiltration, *%*	ATMFI	7.24 ± 1.78	7.73 ± 1.77	6.68 ± 1.62
Posterior thigh muscle-fat infiltration, *%*	PTMFI	10.85 ± 2.33	11.43 ± 2.26	10.18 ± 2.22
Muscle-fat infiltration, *%*	MFI	7.24 ± 1.78	7.73 ± 1.78	6.68 ± 1.62
Weight-to-muscle ratio, *kg/L*	WMR	7.59 ± 1.32	8.34 ± 1.21	6.73 ± 0.82
Abdominal fat ratio, *%*	AFR	0.49 ± 0.11	0.54 ± 0.11	0.44 ± 0.10
Liver proton density fat fraction, *%*	LPDFF	4.03 ± 3.69	3.61 ± 3.49	4.50 ± 4.84
Total thigh muscle volume, *L*	TTMV	10.11 ± 2.52	8.19 ± 1.16	12.32 ± 1.73
Total adipose tissue volume, *L*	TAT	10.43 ± 4.45	10.37 ± 4.55	10.50 ± 4.32
Total abdominal adipose tissue index, L/m^2	TAATi	3.64 ± 1.59	3.90 ± 1.71	3.36 ± 1.38
VAT index, L/m^2	VATi	1.24 ± 0.71	0.98 ± 0.56	1.54 ± 0.73
ASAT index, L/m^2	ASATi	2.42 ± 1.19	2.95 ± 1.25	1.84 ± 0.77
ATMV index, L/m^2	ATMVi	0.59 ± 0.12	0.51 ± 0.07	0.68 ± 0.10
PTMV index, L/m^2	PTMVi	1.63 ± 0.19	1.04 ± 0.12	1.31 ± 0.15
TTMV index, L/m^2	TTMVi	3.50 ± 0.60	3.09 ± 0.36	3.97 ± 0.46
TAT index, L/m^2	TATi	3.67 ± 1.60	3.93 ± 1.73	3.39 ± 1.39
Body composition by bioimpedance				
Body fat, %	BFP	30.85 ± 8.13	35.91 ± 6.63	25.21 ± 5.51
Whole body fat mass, *kg*	BFM	23.50 ± 8.50	25.33 ± 8.95	21.47 ± 7.44
Whole body fat free mass, *kg*	BFFM	52.08 ± 11.03	43.35 ± 4.68	61.79 ± 7.32
Body-mass index body composition, kg/m^2	BMI-BC	26.34 ± 4.23	25.93 ± 4.57	26.80 ± 3.76
Impedance whole body, *Ω*	IWB	609.40 ± 88.94	665.90 ± 72.2	546.60 ± 58.57
Trunk fat, *%*	TFP	30.48 ± 7.59	33.20 ± 7.54	27.45 ± 6.40
Cardiometabolic and anthropometric				
Waist circumference, *cm*	WC	87.77 ± 12.41	82.41 ± 11.61	93.73 ± 10.38
Hip circumference, *cm*	HC	100.60 ± 8.46	100.70 ± 9.52	100.60 ± 7.09
BMI, kg/m^2	BMI	26.32 ± 4.23	25.90 ± 4.57	26.78 ± 3.76
Hand grip strength, *kg*	HG	30.08 ± 10.18	23.04 ± 5.69	37.92 ± 8.14
Pulse, *bpm*	Pulse	68.52 ± 11.93	70.26 ± 11.35	66.59 ± 12.25
Systolic blood pressure, *mmHg*	SBP	140.5 ± 19.66	137.80 ± 20.49	143.40 ± 18.27
Diastolic blood pressure, *mmHg*	DBP	78.67 ± 10.64	76.96 ± 10.57	80.56 ± 10.39
Forced vital capacity, *L*	FVC	3.63 ± 0.93	3.05 ± 0.58	4.30 ± 0.80

Note: Bodily health traits extracted from the UKB, including adipose and muscle tissue from body MRI, body composition by bioimpedance, and cardiometabolic and anthropometric traits from physical examinations. Units are in litres (*L*), kilograms (*kg*), percent (*%*), centimetres (*cm*), height in metres (*m*), ohms (*Ω*), beats per minute (*bpm*), and millimetres of mercury (*mmHg*). For body-brain age prediction, the model was trained with all the listed measures in

combination with the brain MRI features described in section 2.2.

2.4. Age prediction models

Age prediction was carried out using XGBoost regression (eXtreme Gradient Boosting; https://github.com/dmlc/xgboost) in Python 3.8.0, which is based on a decision-tree ensemble algorithm (Chen & Guestrin, 2016) used in several recent age prediction studies (Beck, de Lange, Alnæs, et al., 2022; Beck, de Lange, Pedersen, et al., 2022; Beck et al., 2021; de Lange et al., 2020; Kaufmann et al., 2019; Subramaniapillai et al., 2022; Voldsbekk et al., 2021).

Age prediction models were first run using only brain MRI data for WM and GM features separately. Next, we ran prediction models combining all health traits (overviewed in Table 1) with the brain MRI features per modality. This resulted in four age prediction models used in the current study: T1 brain age, dMRI brain age, T1 body-brain age, and dMRI body-brain age. Additionally, a body age model (see SI Figure 4) using only bodily health traits (i.e., no brain MRI data) was run as a supplement for the purpose of comparison. Parameters were tuned in nested cross-validations with five inner folds for randomised search and 10 outer folds for validating model performance using Scikit-learn (Pedregosa et al., 2011). R^2, root mean squared error (RMSE), mean absolute error (MAE), and Pearson's correlations between predicted and true values were calculated to evaluate prediction accuracy. For each model, 10-fold cross-validation was used to obtain brain age and body-brain age for each individual in the full sample.

2.5. Comparison of age prediction accuracies

To statistically compare the prediction accuracy of the age prediction models of two overlapping samples, we ran Pearson and Filon's z tests for dependent groups, reported as one test in R, version 4.2.0 (www.r-project.org/) (R Core Team, 2022) using the *cocor* function. This test allows us to determine if there's a significant difference between the two correlation coefficients that share a common variable (in this case, the true age). Here, we tested the statistical difference between Pearson's *r* values (correlations coefficients between predicted and true age) for 1) the T1 brain age model and the T1 body-brain age model, 2) the dMRI brain age model and dMRI body-brain age model. The significance threshold was set at $p < 0.05$, and the *p*-values were corrected for multiple comparisons using false discovery rate (FDR) adjustment (Benjamini & Hochberg, 1995).

2.6. Difference in age predictions by bodily health traits

To investigate the degree to which each of the health traits influenced predicted age, Bayesian multilevel models were carried out in *Stan* (Stan Development Team, 2023) using the *brms* (Bürkner, 2017, 2018) R-package, where multivariate models are fitted in familiar syntax to comparable frequentist approaches such as a linear mixed effects model using the *lme4* (Bates et al., 2015).

We assessed the relationships between age prediction difference scores (predicted body-brain age minus predicted brain age) and each health trait (bar body MRI index scores to reduce redundancy). The age prediction difference score (for T1 and dMRI separately) was entered as the dependent variable, with each health trait separately entered as the independent fixed effects variable along with age and sex, with subject ID as the random effect:

$$Age\ prediction\ difference\ score \sim Health\ trait + Age + Sex\ (1|SubjectID) \qquad (1)$$

To prevent false positives and to regularise the estimated associations, we defined a standard prior around zero with a standard deviation of 1 for all coefficients. All variables bar sex were standardised before running the analyses. For each coefficient of interest, we report the mean estimated value of the posterior distribution (β) and its 95% credible interval (the range of values that with 95% confidence contains the true value of the association), and calculated the Bayes Factor (BF) – provided as evidence ratios in the presented figures – using the Savage-Dickey method (Wagenmakers et al., 2010). Briefly, BF can be interpreted as a measure of the strength of evidence (*extreme, very strong, strong, moderate, anecdotal, none*) in favour of the null or alternative hypothesis. For a pragmatic guide on BF interpretation, see SI Table 1.

3. Results

3.1. Brain age and body-brain age prediction

Table 2 summarises descriptive and model validation statistics pertaining to each age prediction model. Figure 1 shows the age difference score distributions of the brain age vs body-brain age models. SI Figure 5 shows the correlation between the brain age vs body-brain age difference scores. Figure 2 shows a correlation matrix including the four models' predicted ages. See SI Figures 6 and 7 for correlation matrices showing the association between health traits, SI Figure 8 for predicted age as a function of chronological age for

each age prediction model, and SI Figure 9 for a correlation matrix including all the brain-age and body-brain-age gaps for each of the four models.

Table 2. Correlations between predicted and true age (*r*) and confidence intervals, average R^2, root mean square error (RMSE), and mean absolute error (MAE) standard deviation for each age prediction model.

		Brain age model	**Body-brain age model**
dMRI	*r*	0.77 [0.77-0.77]	0.82 [0.82-0.83]
	R^2	0.62 ± 0.01	0.67 ± 0.01
	RMSE	4.67 ± 0.12	4.24 ± 0.06
	MAE	3.70 ± 0.07	3.39 ± 0.06
T1	*r*	0.76 [0.76-0.76]	0.80 [0.80-0.81]
	R^2	0.57 ± 0.02	0.64 ± 0.01
	RMSE	4.93 ± 0.06	4.52 ± 0.07
	MAE	3.94 ± 0.05	3.57 ± 0.06

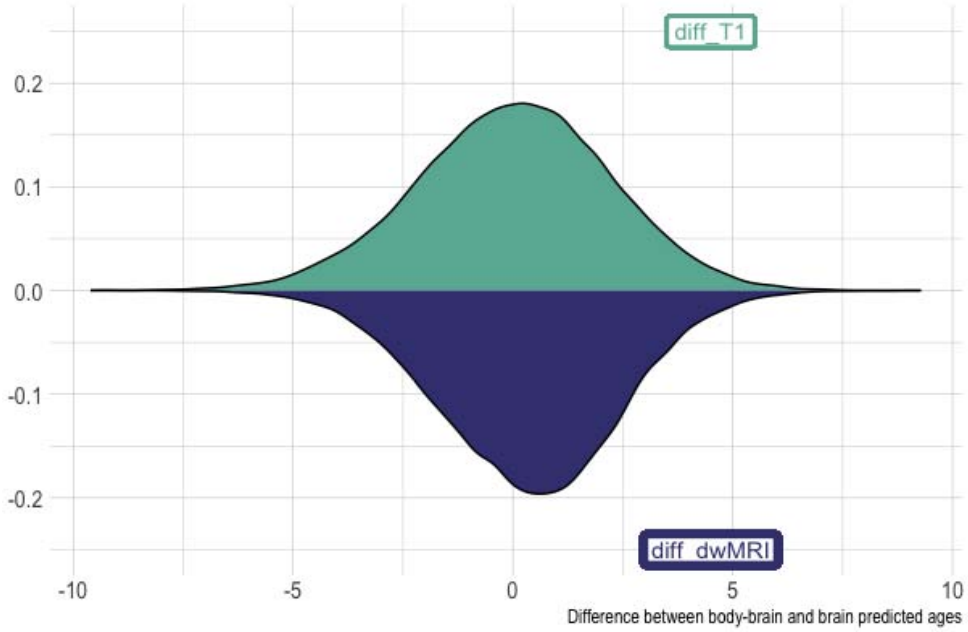

Figure 1. Age difference score distribution (density) for T1 (diff_T1) and dMRI (diff_dwMRI) weighted age models. Mean difference scores = .004 (T1) and 3.57 (dMRI), with standard deviation (SD) of 2.22 and 2.06,

respectively. The SDs indicate that the shifts in individual age predictions when adding health traits ranged up to ± 2 years.

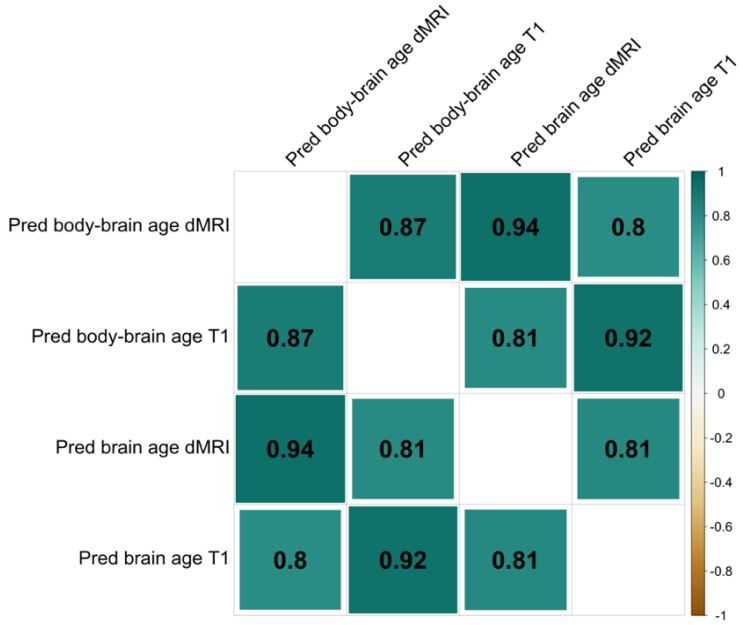

Figure 2. Correlation matrix showing the associations between the predicted ages of the four models.

3.2. Statistical differences between the models

Pearson and Filon s z tests revealed a statistically significant difference in predicted age between the brain age and body-brain age models, including differences between the T1 brain age and T1 body-brain age models (z = -34.4, $p < .01$) and the dMRI brain age and dMRI body-brain age models (z = -44.6 , $p < .01$).

3.3. Bayesian multilevel models

Bayesian multilevel modelling tested the associations between each bodily health trait and the difference score (body-brain predicted age minus brain predicted age). Due to the large number of included health traits, we present associations between 1) age prediction difference and body MRI measures and 2) age prediction difference and cardiometabolic, anthropometric and bioimpedance measures separately below. The full results are available in SI Tables 2 and 3. For estimated credible intervals, see SI Figures 10 and 11. See SI Table 4 for full and partial linear regressions between age and each of the health trait adjusted for brain-predicted age.

3.3.1. Age difference scores and body MRI features

Figure 3 shows posterior distributions reflecting the associations between each body MRI feature and the age difference score between brain-age vs body-brain-age models. Values increasing from 0 to 1 indicate evidence of a positive association and values decreasing 0 to -1 indicate evidence of a negative association.

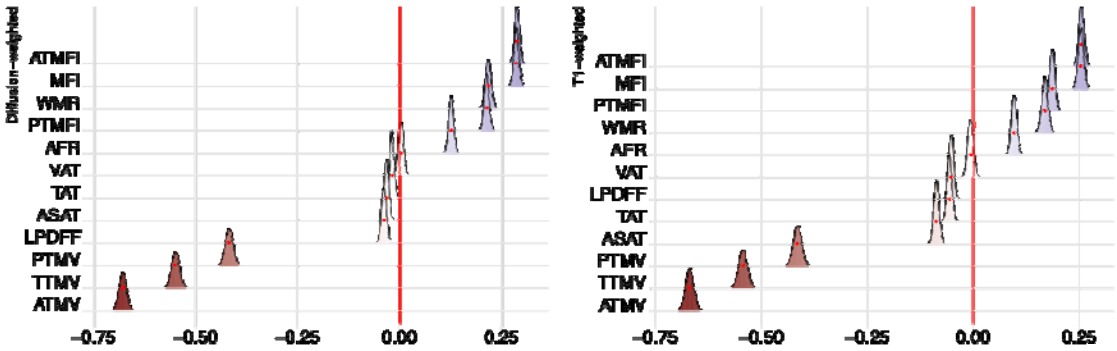

Figure 3. Associations between body MRI features and difference scores between brain-age models and body-brain-age models (dMRI and T1). The figure shows posterior distributions of the estimates of the standardised coefficient. Estimates for each body MRI feature on dMRI difference score on the left and T1-weighted difference score on the right. Colour scale follows the directionality of evidence, with positive (blue) values indicating evidence in favour of positive associations and negative (red) values indicating evidence in favour of negative associations. The width of the distribution represents the uncertainty of the parameter estimates. For a list of unabbreviated words, see Table 1.

For the T1 age difference scores, the tests revealed extreme evidence of a positive association with predicted age difference score (calculated as T1 body-brain age – T1 brain age) for ATMFI (BF = 0, β = 0.24), PTMFI (BF = 0, β = 0.19), MFI (BF = 0, β = 0.25), WMR (BF = 0, β = 0.17), and AFR (BF = 0, β = 0.10), indicating that higher levels of muscle-fat infiltration in the thighs, high weight-to-muscle ratio, and high abdominal fat (ratio measure), are associated with a positive difference score, i.e., higher predicted body-brain age than brain age.

The tests also revealed extreme evidence of a negative association with predicted age difference score for ASAT (BF = 0, β = -0.09), ATMV (BF = 0, β = -0.67), PTMV (BF = 0, β = -0.41), LPDFF (BF = 0, β = -0.05), TTMV (BF = 0, β = -0.54), and TAT (BF = 0, β = -0.06), indicating that higher liver fat, muscle volume, subcutaneous and total fat were associated with a negative difference score, i.e., lower predicted body-brain age than brain age. There was also extreme evidence favouring no association for VAT (BF = 84.9, β = 0.01).

For the dMRI age difference scores, the tests revealed extreme evidence of a positive association with predicted age difference score (dMRI body-brain age – dMRI brain age) for ATMFI (BF = 0, β = 0.29), PTMFI (BF = 0, β = 0.21), MFI (BF = 0, β = 0.29), WMR (BF = 0, β = 0.22), and AFR (BF = 0, β = 0.13), indicating that muscle-fat infiltration in the thighs, high weight-to-muscle ratio, and high abdominal fat, is associated with a positive difference score, i.e., higher predicted body-brain age than brain age.

The tests also revealed extreme evidence in favour of a negative association with predicted age difference score for ASAT (BF = 0, β = -0.03), ATMV (BF = 0, β = -0.68), PTMV (BF = 0, β = -0.42), LPDFF (BF = 0, β = -0.04), TTMV (BF = 0, β = -0.55), and moderate evidence for TAT (BF = 0.28, β = -0.02), indicating that higher liver fat, muscle volume, subcutaneous and total body fat were associated with a negative difference score, i.e., lower predicted body-brain age than brain age.

Lastly, the tests revealed extreme evidence of no association with the predicted age difference score for VAT (BF = 146.2, β = 0.00). Based on the beta coefficients, measures related to muscle volume (ATMV, PTMV, TTMV) showed greater associations with the age difference scores than measures related to adipose tissue (LPDFF, TAT, and VAT).

3.3.2. Age difference scores and cardiometabolic, anthropometric and bioimpedance traits

Figure 4 shows posterior distributions reflecting the associations between cardiometabolic, anthropometric, and bioimpedance traits and the difference score between brain age vs body-brain age models.

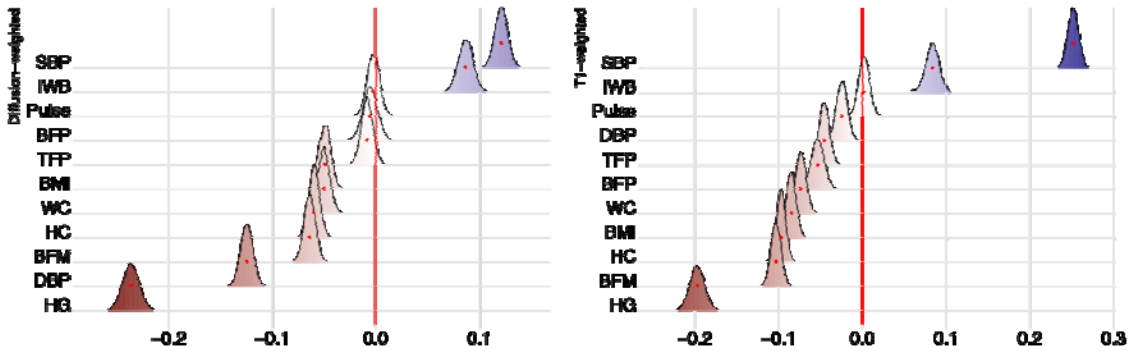

Figure 4. Associations between cardiometabolic, anthropometric, and bioimpedance traits and difference score between brain age models and body-brain age models (dMRI and T1). The figure shows posterior distributions of the estimates of the standardised coefficient. Estimates for each health trait on dMRI difference score on the left and T1-weighted difference score on the right. Colour scale follows directionality of evidence,

with positive (blue) values indicating evidence in favour of positive associations and negative (red) values indicating evidence in favour of negative associations. Width of the distribution represents the uncertainty of the parameter estimates. Table 1 presents a list of unabbreviated words.

For the T1 age difference scores, the tests revealed extreme evidence in favour of a positive association with predicted age difference score (T1 body-brain age – T1 brain age) for SBP (BF = 0, β = 0.25) and IWB (BF = 0, β = 0.08), indicating that high systolic blood pressure and high impedance (i.e., low muscle volume) were associated with a positive difference score, i.e., higher predicted body-brain age than brain age.

The tests also revealed extreme evidence in favour of a negative association with predicted age difference score for WC (BF = 0, β = -0.07), HC (BF = 0, β = -0.10), BFP (BF = 0, β = -0.05), HG (BF = 0, β = -0.20), BFM (BF = 0, β = -0.10), TFP (BF = 0, β = -0.05), and BMI (BF = 0, β = -0.09), and moderate evidence for DBP (BF = 0.11, β = -0.03), indicating that higher hand grip strength and poorer cardiometabolic and anthropometric health are associated with a negative difference score, i.e., higher predicted brain age than body-brain age.

Additionally, the tests revealed extreme evidence in favour of no association with predicted age difference score for pulse (BF = 155.4, β = 0.00), indicating that pulse rate was not associated with a higher or lower difference score in predicted age between the models.

For the dMRI age difference scores, the tests revealed extreme evidence of a positive association with predicted age difference score (dMRI body-brain age – dMRI brain age) for SBP (BF = 0, β = 0.12) and IWB (BF = 0, β = 0.09), indicating that high systolic blood pressure and high impendence (low muscle volume) were associated with a positive difference score, i.e., higher predicted body-brain age than brain age.

The tests also revealed extreme evidence of a negative association with predicted age difference score for WC (BF = 0, β = -0.05), HC (BF = 0, β = -0.06), DBP (BF = 0, β = -0.13), HG (BF = 0, β = -0.24), BFM (BF = 0, β = -0.06), BMI (BF = 0, β = -0.05), indicating that higher hand grip strength and poorer cardiometabolic and anthropometric health were associated with a negative difference score, i.e., higher predicted brain age than body-brain age.

Moreover, the tests revealed extreme evidence in favour of no association for pulse rate (BF = 154.7, β = -0.00), BFP (BF = 100.4, β = -0.01), and TFP (BF = 55.4, β = -0.01). Based on the beta coefficients, measures related to hand grip strength (HG) and total adipose measures (HC, BFM, and BMI) showed strong associations with T1 and dMRI age difference

scores. In contrast, beta coefficients for cardiometabolic health (WC, DPB, BFP, and TFP) were smaller, as highlighted in Figure 4.

4. Discussion

Evidence of differential ageing rates across different biological systems in the same individual (Cevenini et al., 2008) has led us to conceptualise ageing as a mosaic and heterogeneous construct. One implication is that individual biomarkers studied in isolation may not accurately reflect risk of disease or outcome (Sebastiani et al., 2017), and the use of multiple models in coherence has been recommended (Cevenini et al., 2008; Cole et al., 2019; Kuo et al., 2021). Our analyses revealed that including bodily health traits in the age prediction models rendered significantly higher accuracy of age prediction compared to the models trained solely on brain MRI data. Multilevel modelling showed that relative to the predictions based only on brain MRI, several elevated body health risks contributed to a group-level increase in predicted age, while markers suggestive of muscular fitness contributed to a decrease in predicted age. Hence, combining health traits with brain imaging features may provide valuable information for understanding the unique and common variance across body and brain health indicators.

In the prediction models, the estimated age varied by approximately 4 years across the whole sample for a given true age. The shifts in individual predictions when adding the health traits to the models ranged up to ± 6 years, indicating relatively large changes for some individuals compared to the group-level MAEs. Moreover, the analyses revealed that the standard deviations of the mean brain-predicted age and body-brain-predicted age difference score distributions shifted up to ± 2 years in individual age predictions when adding health traits, indicating increased variance when adding health traits to the models. Further, the correlation (SI Figure 4) between the difference scores in T1- and dMRI-based models indicate that the changes in predictions introduced by health traits are related but not identical. These shifts suggest that health traits in some individuals are sensitive to the age-related variance not captured by brain imaging data, indicating heterogeneous ageing rates across biological systems and individuals.

An individual may have a brain-predicted age closely aligned with their chronological age but a body-brain age that exceeds it. One theoretical explanation for this is involvement of brain maintenance or reserve (Anatürk et al., 2021; Nyberg, 2017), where brain health is to some extent preserved irrespective of bodily health status. Future studies may therefore

aim to investigate these difference scores in the context of reserve-related mechanisms, including individual factors such as education, socioeconomic status, and societal factors such as access to health care. Although speculative, higher body-brain age than brain age may also reflect worsening bodily health that has not yet manifested in the brain, which may represent a window of opportunity for intervention. This emphasises the importance of future longitudinal studies.

To better interpret the differences between the body-brain and brain age predictions, we ran Bayesian multilevel modelling to measure the association between the predicted age difference score and each of the health traits. The results showed that measures related to higher systolic blood pressure and higher muscle-fat infiltration, especially in the thighs, were related to a positive difference score, i.e., higher predicted body-brain age than predicted brain age. Conversely, higher hand-grip strength, and muscle volume (especially in the thighs), were related to a negative difference score, i.e., lower predicted body-brain age than predicted brain age. These results are in line with our expectations of measures related to poorer and better somatic health having differential contributions to our age models, whereby poor health is manifested as older appearing predicted age and good health as younger appearing. This is also supported by previous literature linking higher muscle infiltration, systolic blood pressure, and weaker grip strength to older-looking brains (Beck, de Lange, Alnæs, et al., 2022; Beck, de Lange, Pedersen, et al., 2022; Cole et al., 2018; de Lange et al., 2020) and higher muscle volume with younger-looking brains (Beck, de Lange, Alnæs, et al., 2022).

Despite abdominal fat ratio being related to a positive difference score, several other measures related to body fat, including subcutaneous and total fat, BMI, WC, and HC were associated with either a negative difference score or no effect. Previous research has also reported inconsistent effects for adipose-related measures and brain age (Beck, de Lange, Alnæs, et al., 2022; Beck, de Lange, Pedersen, et al., 2022), including opposite trends for systolic and diastolic blood pressure, as found in our study. In light of our expectations, these findings are counterintuitive and do not support our hypotheses. Although speculative, the potentially conflicting results may be explained by the demographics of our study, consisting of mid-to-late-life participants in a generally healthy population. It could be the case that the sample investigated does not represent individuals that have high cardiovascular risk in mid-life due to cardiovascular-related deaths before senescence and thus skewing the representativeness of the sample. Another contributing factor could be the potentially beneficial impact of abdominal adipose tissue on brain health in females. For example,

previous research has indicated that among women aged 66-96, an increase in abdominal subcutaneous fat correlates with reduced dementia risk (Spauwen et al., 2017). The associations observed for abdominal adiposity in our study might be slightly driven by these female-specific effects in a combined sample of males and females. However, future research is needed to confirm this speculation. Longitudinally designed studies with several waves are needed to better understand the potentially counterintuitive directionality of some health traits used in the current study.

Although previous studies have demonstrated that variation in predicted brain age is partly explained by individual differences in body composition and health traits, including abdominal fat (Beck, de Lange, Pedersen, et al., 2022; Schindler et al., 2022; Subramaniapillai et al., 2022), muscle-fat infiltration (Beck, de Lange, Alnæs, et al., 2022), hand-grip strength (Cole et al., 2018; Sanders et al., 2021) and muscle volume (Beck, de Lange, Alnæs, et al., 2022), our findings suggest that these health traits may influence age predictions beyond what is captured by the brain imaging measures. The relative contribution of the health status of each individual not only influences the direction of the effect on brain health but also contributes to the accuracy of the age prediction models themselves, providing a more accurate depiction of biological ageing.

Some strengths and limitations of the study must be discussed. The UK Biobank offers a rich and comprehensive dataset with a large population robust for analysis. Moreover, it offers a wide range of health-related information, including lifestyle and health factors utilised in the current study. It is, however, important to note that volunteer samples such as the UK Biobank are limited by selection biases such as healthy-volunteer bias (Brayne & Moffitt, 2022; Tyrrell et al., 2021), overall relatively higher education, and overrepresentation by individuals of white European descent, making the sample less representative of the wider population. One argument in favour of recruiting healthy individuals at baseline is that some will develop illnesses over the course of the study period, allowing researchers to track changes over time and identify predictors of health decline and therefore targets for intervention strategies. A further limitation of the UK Biobank is the limited age range, with participants involved being between 44-82 years of age. Given the importance of tracking changes over time and the potential differences in how bodily health traits may relate to brain health across the lifespan (Kivimäki et al., 2018), and that this may also vary between males and females (Subramaniapillai et al., 2022), future research should include wide age ranges, preferably including longitudinal data on more diverse and representative samples.

To summarise, we found that adding bodily health traits significantly improved age prediction accuracy compared to using brain MRI data alone, and that specific health traits may influence age predictions beyond what is captured by the brain imaging measures. Our results emphasise the importance of considering both body and brain measures for a more comprehensive understanding of biological ageing. The current study thus contributes to the dissection of the unique and common variance across body and brain health indicators, which is key towards the aim of parsing inter-individual heterogeneity in the multisystem ageing process. Future research should attempt to better understand the clinical relevance of individual-level discrepancies between different age prediction models in relation to early life exposures, lifestyle factors, genetic architecture, and their relation to risk for cardiovascular disease and age-related neurodegenerative and cognitive disorders.

5. Data availability

The UK Biobank resource is open for eligible researchers upon application (http://www.ukbiobank.ac.uk/register-apply/).

6. Acknowledgements

The Research Council of Norway (#223273, #324252, #300767, #324499); South-Eastern Norway Regional Health Authority (#2017112; #2019101, #2022080, #2020060); European Union's Horizon 2020 Research and Innovation Programme (CoMorMent project, Grant #847776; BRAINMINT project, Grant #802998), and the German Federal Ministry of Education and Research (BMBF, grant 01ZX1904A). We performed this work on the *Services for sensitive data* (TSD), University of Oslo, Norway, with resources provided by UNINETT Sigma2 - the National Infrastructure for High-Performance Computing and Data Storage in Norway. We conducted this research using the UK Biobank Resource under Application Number 27412.

7. Conflicts of interest

OAA is a consultant to cortechs.ai and received speaker's honorarium from Lundbeck, Janssen and Sunovion unrelated to the topic of the current study. JL is an employee and shareholder of AMRA Medical AB and reports consulting and speaking honoraria from Eli Lilly and BioMarin unrelated to the topic of the current study. ODL is an employee and shareholder of AMRA Medical AB and reports consulting from Eli Lilly and Fulcrum Therapeutics unrelated to the topic of the current study.

8. References

Alfaro, F. J., Gavrieli, A., Saade-Lemus, P., Lioutas, V.-A., Upadhyay, J., & Novak, V. (2018). White matter microstructure and cognitive decline in metabolic syndrome: A review of diffusion tensor imaging. *Metabolism: Clinical and Experimental*, *78*, 52–68. https://doi.org/10.1016/j.metabol.2017.08.009

Anatürk, M., Kaufmann, T., Cole, J. H., Suri, S., Griffanti, L., Zsoldos, E., Filippini, N., Singh-Manoux, A., Kivimäki, M., Westlye, L. T., Ebmeier, K. P., & Lange, A.-M. G. de. (2021). Prediction of brain age and cognitive age: Quantifying brain and cognitive maintenance in aging. *Human Brain Mapping*, *42*(6), 1626–1640. https://doi.org/10.1002/hbm.25316

Basser, P. J. (1995). Inferring microstructural features and the physiological state of tissues from diffusion-weighted images. *NMR in Biomedicine*, *8*(7), 333–344. https://doi.org/10.1002/nbm.1940080707

Bates, D., Mächler, M., Bolker, B., & Walker, S. (2015). Fitting Linear Mixed-Effects Models Using lme4. *Journal of Statistical Software*, *67*(1). https://doi.org/10.18637/jss.v067.i01

Beck, D., de Lange, A.-M. G., Alnæs, D., Maximov, I. I., Pedersen, M. L., Leinhard, O. D., Linge, J., Simon, R., Richard, G., Ulrichsen, K. M., Dørum, E. S., Kolskår, K. K., Sanders, A.-M., Winterton, A., Gurholt, T. P., Kaufmann, T., Steen, N. E., Nordvik, J. E., Andreassen, O. A., & Westlye, L. T. (2022). Adipose tissue distribution from body MRI is associated with cross-sectional and longitudinal brain age in adults. *NeuroImage: Clinical*, *33*, 102949. https://doi.org/10.1016/j.nicl.2022.102949

Beck, D., de Lange, A.-M. G., Maximov, I. I., Richard, G., Andreassen, O. A., Nordvik, J. E., & Westlye, L. T. (2021). White matter microstructure across the adult lifespan: A mixed longitudinal and cross-sectional study using advanced diffusion models and

brain-age prediction. *NeuroImage*, *224*, 117441. https://doi.org/10.1016/j.neuroimage.2020.117441

Beck, D., de Lange, A.-M. G., Pedersen, M. L., Alnæs, D., Maximov, I. I., Voldsbekk, I., Richard, G., Sanders, A.-M., Ulrichsen, K. M., Dørum, E. S., Kolskår, K. K., Høgestøl, E. A., Steen, N. E., Djurovic, S., Andreassen, O. A., Nordvik, J. E., Kaufmann, T., & Westlye, L. T. (2022). Cardiometabolic risk factors associated with brain age and accelerate brain ageing. *Human Brain Mapping*, *43*(2), 700–720. https://doi.org/10.1002/hbm.25680

Benjamini, Y., & Hochberg, Y. (1995). Controlling the False Discovery Rate: A Practical and Powerful Approach to Multiple Testing. *Journal of the Royal Statistical Society: Series B (Methodological)*, *57*(1), 289–300. https://doi.org/10.1111/j.2517-6161.1995.tb02031.x

Borga, M., Ahlgren, A., Romu, T., Widholm, P., Dahlqvist Leinhard, O., & West, J. (2020). Reproducibility and repeatability of MRI-based body composition analysis. *Magnetic Resonance in Medicine*, *84*(6), 3146–3156. https://doi.org/10.1002/mrm.28360

Borga, M., West, J., Bell, J. D., Harvey, N. C., Romu, T., Heymsfield, S. B., & Dahlqvist Leinhard, O. (2018). Advanced body composition assessment: From body mass index to body composition profiling. *Journal of Investigative Medicine: The Official Publication of the American Federation for Clinical Research*, *66*(5), 1–9. https://doi.org/10.1136/jim-2018-000722

Brain, J., Greene, L., Tang, E. Y. H., Louise, J., Salter, A., Beach, S., Turnbull, D., Siervo, M., Stephan, B. C. M., & Tully, P. J. (2023). Cardiovascular disease, associated risk factors, and risk of dementia: An umbrella review of meta-analyses. *Frontiers in Epidemiology*, *3*. https://www.frontiersin.org/articles/10.3389/fepid.2023.1095236

Brayne, C., & Moffitt, T. E. (2022). The limitations of large-scale volunteer databases to address inequalities and global challenges in health and aging. *Nature Aging*, *2*(9), Article 9. https://doi.org/10.1038/s43587-022-00277-x

Bürkner, P.-C. (2017). **brms**: An *R* Package for Bayesian Multilevel Models Using *Stan*. *Journal of Statistical Software*, *80*(1). https://doi.org/10.18637/jss.v080.i01

Bürkner, P.-C. (2018). Advanced Bayesian Multilevel Modeling with the R Package brms. *The R Journal*, *10*(1), 395. https://doi.org/10.32614/RJ-2018-017

Cevenini, E., Invidia, L., Lescai, F., Salvioli, S., Tieri, P., Castellani, G., & Franceschi, C. (2008). Human models of aging and longevity. *Expert Opinion on Biological Therapy*, *8*(9), 1393–1405. https://doi.org/10.1517/14712598.8.9.1393

Chen, T., & Guestrin, C. (2016). XGBoost: A Scalable Tree Boosting System. *Proceedings of the 22nd ACM SIGKDD International Conference on Knowledge Discovery and Data Mining*, 785–794. https://doi.org/10.1145/2939672.2939785

Cole, & Franke, K. (2017). Predicting Age Using Neuroimaging: Innovative Brain Ageing Biomarkers. *Trends in Neurosciences*, *40*(12), 681–690. https://doi.org/10.1016/j.tins.2017.10.001

Cole, J. H., Marioni, R. E., Harris, S. E., & Deary, I. J. (2019). Brain age and other bodily ‘ages’: Implications for neuropsychiatry. *Molecular Psychiatry*, *24*(2), 266–281. https://doi.org/10.1038/s41380-018-0098-1

Cole, J. H., Poudel, R. P. K., Tsagkrasoulis, D., Caan, M. W. A., Steves, C., Spector, T. D., & Montana, G. (2017). Predicting brain age with deep learning from raw imaging data results in a reliable and heritable biomarker. *NeuroImage*, *163*, 115–124. https://doi.org/10.1016/j.neuroimage.2017.07.059

Cole, J. H., Ritchie, S. J., Bastin, M. E., Hernández, M. C. V., Maniega, S. M., Royle, N., Corley, J., Pattie, A., Harris, S. E., Zhang, Q., Wray, N. R., Redmond, P., Marioni, R.

E., Starr, J. M., Cox, S. R., Wardlaw, J. M., Sharp, D. J., & Deary, I. J. (2018). Brain age predicts mortality. *Molecular Psychiatry*, *23*(5), 1385–1392. https://doi.org/10.1038/mp.2017.62

Collins, R. (2007). *UK Biobank Protocol*.

de Lange, A.-M. G., Anatürk, M., Suri, S., Kaufmann, T., Cole, J. H., Griffanti, L., Zsoldos, E., Jensen, D. E. A., Filippini, N., Singh-Manoux, A., Kivimäki, M., Westlye, L. T., & Ebmeier, K. P. (2020). Multimodal brain-age prediction and cardiovascular risk: The Whitehall II MRI sub-study. *NeuroImage*, *222*, 117292. https://doi.org/10.1016/j.neuroimage.2020.117292

de Lange, A.-M. G., Kaufmann, T., van der Meer, D., Maglanoc, L. A., Alnæs, D., Moberget, T., Douaud, G., Andreassen, O. A., & Westlye, L. T. (2019). Population-based neuroimaging reveals traces of childbirth in the maternal brain. *Proceedings of the National Academy of Sciences*, *116*(44), 22341–22346. https://doi.org/10.1073/pnas.1910666116

Fieremans, E., Jensen, J. H., & Helpern, J. A. (2011). White matter characterization with diffusional kurtosis imaging. *NeuroImage*, *58*(1), 177–188. https://doi.org/10.1016/j.neuroimage.2011.06.006

Fischl, B., Salat, D. H., Busa, E., Albert, M., Dieterich, M., Haselgrove, C., van der Kouwe, A., Killiany, R., Kennedy, D., Klaveness, S., Montillo, A., Makris, N., Rosen, B., & Dale, A. M. (2002). Whole Brain Segmentation. *Neuron*, *33*(3), 341–355. https://doi.org/10.1016/S0896-6273(02)00569-X

Franke, K., Gaser, C., Manor, B., & Novak, V. (2013). Advanced BrainAGE in older adults with type 2 diabetes mellitus. *Frontiers in Aging Neuroscience*, *5*. https://doi.org/10.3389/fnagi.2013.00090

Franke, K., Ristow, M., & Gaser, C. (2014). Gender-specific impact of personal health parameters on individual brain aging in cognitively unimpaired elderly subjects. *Frontiers in Aging Neuroscience*, *6*. https://doi.org/10.3389/fnagi.2014.00094

Franke, K., Ziegler, G., Klöppel, S., & Gaser, C. (2010). Estimating the age of healthy subjects from T1-weighted MRI scans using kernel methods: Exploring the influence of various parameters. *NeuroImage*, *50*(3), 883–892. https://doi.org/10.1016/j.neuroimage.2010.01.005

Glasser, M. F., Coalson, T. S., Robinson, E. C., Hacker, C. D., Harwell, J., Yacoub, E., Ugurbil, K., Andersson, J., Beckmann, C. F., Jenkinson, M., Smith, S. M., & Van Essen, D. C. (2016). A multi-modal parcellation of human cerebral cortex. *Nature*, *536*(7615), Article 7615. https://doi.org/10.1038/nature18933

Jensen, J. H., Helpern, J. A., Ramani, A., Lu, H., & Kaczynski, K. (2005). Diffusional kurtosis imaging: The quantification of non-gaussian water diffusion by means of magnetic resonance imaging. *Magnetic Resonance in Medicine*, *53*(6), 1432–1440. https://doi.org/10.1002/mrm.20508

Kaden, E., Kelm, N. D., Carson, R. P., Does, M. D., & Alexander, D. C. (2016). Multi-compartment microscopic diffusion imaging. *NeuroImage*, *139*, 346–359. https://doi.org/10.1016/j.neuroimage.2016.06.002

Karlsson, A., Rosander, J., Romu, T., Tallberg, J., Grönqvist, A., Borga, M., & Dahlqvist Leinhard, O. (2015). Automatic and quantitative assessment of regional muscle volume by multi-atlas segmentation using whole-body water-fat MRI. *Journal of Magnetic Resonance Imaging: JMRI*, *41*(6), 1558–1569. https://doi.org/10.1002/jmri.24726

Kaufmann, T., van der Meer, D., Doan, N. T., Schwarz, E., Lund, M. J., Agartz, I., Alnæs, D., Barch, D. M., Baur-Streubel, R., Bertolino, A., Bettella, F., Beyer, M. K., Bøen,

E., Borgwardt, S., Brandt, C. L., Buitelaar, J., Celius, E. G., Cervenka, S., Conzelmann, A., … Westlye, L. T. (2019). Common brain disorders are associated with heritable patterns of apparent aging of the brain. *Nature Neuroscience*, *22*(10), Article 10. https://doi.org/10.1038/s41593-019-0471-7

Kivimäki, M., Luukkonen, R., Batty, G. D., Ferrie, J. E., Pentti, J., Nyberg, S. T., Shipley, M. J., Alfredsson, L., Fransson, E. I., Goldberg, M., Knutsson, A., Koskenvuo, M., Kuosma, E., Nordin, M., Suominen, S. B., Theorell, T., Vuoksimaa, E., Westerholm, P., Westerlund, H., … Jokela, M. (2018). Body mass index and risk of dementia: Analysis of individual-level data from 1.3 million individuals. *Alzheimer's & Dementia*, *14*(5), 601–609. https://doi.org/10.1016/j.jalz.2017.09.016

Kolenic, M., Franke, K., Hlinka, J., Matejka, M., Capkova, J., Pausova, Z., Uher, R., Alda, M., Spaniel, F., & Hajek, T. (2018). Obesity, dyslipidemia and brain age in first-episode psychosis. *Journal of Psychiatric Research*, *99*, 151–158. https://doi.org/10.1016/j.jpsychires.2018.02.012

Kuo, C.-Y., Tai, T.-M., Lee, P.-L., Tseng, C.-W., Chen, C.-Y., Chen, L.-K., Lee, C.-K., Chou, K.-H., See, S., & Lin, C.-P. (2021). Improving Individual Brain Age Prediction Using an Ensemble Deep Learning Framework. *Frontiers in Psychiatry*, *12*, 308. https://doi.org/10.3389/fpsyt.2021.626677

Leonardsen, E. H., Peng, H., Kaufmann, T., Agartz, I., Andreassen, O. A., Celius, E. G., Espeseth, T., Harbo, H. F., Høgestøl, E. A., Lange, A.-M. de, Marquand, A. F., Vidal-Piñeiro, D., Roe, J. M., Selbæk, G., Sørensen, Ø., Smith, S. M., Westlye, L. T., Wolfers, T., & Wang, Y. (2022). Deep neural networks learn general and clinically relevant representations of the ageing brain. *NeuroImage*, *256*, 119210. https://doi.org/10.1016/j.neuroimage.2022.119210

Linge, J., Borga, M., West, J., Tuthill, T., Miller, M. R., Dumitriu, A., Thomas, E. L., Romu, T., Tunón, P., Bell, J. D., & Dahlqvist Leinhard, O. (2018). Body Composition Profiling in the UK Biobank Imaging Study: Body Composition Profiling in UK Biobank. *Obesity*, *26*(11), 1785–1795. https://doi.org/10.1002/oby.22210

López-Otín, C., Blasco, M. A., Partridge, L., Serrano, M., & Kroemer, G. (2013). The Hallmarks of Aging. *Cell*, *153*(6), 1194–1217. https://doi.org/10.1016/j.cell.2013.05.039

Massy-Westropp, N. M., Gill, T. K., Taylor, A. W., Bohannon, R. W., & Hill, C. L. (2011). Hand Grip Strength: Age and gender stratified normative data in a population-based study. *BMC Research Notes*, *4*, 127. https://doi.org/10.1186/1756-0500-4-127

Maximov, I. I., Alnæs, D., & Westlye, L. T. (2019). Towards an optimised processing pipeline for diffusion magnetic resonance imaging data: Effects of artefact corrections on diffusion metrics and their age associations in UK Biobank. *Human Brain Mapping*, *40*(14), 4146–4162. https://doi.org/10.1002/hbm.24691

Maximov, I. I., van der Meer, D., de Lange, A.-M. G., Kaufmann, T., Shadrin, A., Frei, O., Wolfers, T., & Westlye, L. T. (2021). Fast qualitY conTrol meThod foR derIved diffUsion Metrics (YTTRIUM) in big data analysis: U.K. Biobank 18,608 example. *Human Brain Mapping*, *42*(10), 3141–3155. https://doi.org/10.1002/hbm.25424

Maximov, I. I., van der Meer, D., de Lange, A.-M., Kaufmann, T., Shadrin, A., Frei, O., Wolfers, T., & Westlye, L. T. (2020). *Fast qualit **Y** con **T** rol me **T** hod fo **R** der **I** ved diff **U** sion **M** etrics (**YTTRIUM**) in big data analysis: UK Biobank 18608 example* [Preprint]. Neuroscience. https://doi.org/10.1101/2020.02.17.952697

Mielke, M. M., Bandaru, V. V. R., Haughey, N. J., Rabins, P. V., Lyketsos, C. G., & Carlson, M. C. (2010). Serum sphingomyelins and ceramides are early predictors of memory

impairment. *Neurobiology of Aging*, *31*(1), 17–24. https://doi.org/10.1016/j.neurobiolaging.2008.03.011

Miller, K. L., Alfaro-Almagro, F., Bangerter, N. K., Thomas, D. L., Yacoub, E., Xu, J., Bartsch, A. J., Jbabdi, S., Sotiropoulos, S. N., Andersson, J. L. R., Griffanti, L., Douaud, G., Okell, T. W., Weale, P., Dragonu, I., Garratt, S., Hudson, S., Collins, R., Jenkinson, M., … Smith, S. M. (2016). Multimodal population brain imaging in the UK Biobank prospective epidemiological study. *Nature Neuroscience*, *19*(11), 1523–1536. https://doi.org/10.1038/nn.4393

Mori, S., Wakana, Nagae-Poetscher, & van Zijl, P. C. M. (2006). MRI Atlas of Human White Matter. *AJNR: American Journal of Neuroradiology*, *27*(6), 1384–1385.

Nyberg, L. (2017). Neuroimaging in aging: Brain maintenance. *F1000Research*, *6*, 1215. https://doi.org/10.12688/f1000research.11419.1

Pedregosa, F., Varoquaux, G., Gramfort, A., Michel, V., Thirion, B., Grisel, O., Blondel, M., Prettenhofer, P., Weiss, R., Dubourg, V., Vanderplas, J., Passos, A., Cournapeau, D., Brucher, M., Perrot, M., & Duchesnay, É. (2011). Scikit-learn: Machine Learning in Python. *The Journal of Machine Learning Research*, *12*(null), 2825–2830.

R Core Team. (2022). *R: A Language and Environment for Statistical Computing*. R Foundation for Statistical Computing. https://www.R-project.org/

Rodgers, J. L., Jones, J., Bolleddu, S. I., Vanthenapalli, S., Rodgers, L. E., Shah, K., Karia, K., & Panguluri, S. K. (2019). Cardiovascular Risks Associated with Gender and Aging. *Journal of Cardiovascular Development and Disease*, *6*(2), Article 2. https://doi.org/10.3390/jcdd6020019

Ronan, L., Alexander-Bloch, A. F., Wagstyl, K., Farooqi, S., Brayne, C., Tyler, L. K., & Fletcher, P. C. (2016). Obesity associated with increased brain age from midlife.

Neurobiology of Aging, *47*, 63–70. https://doi.org/10.1016/j.neurobiolaging.2016.07.010

Sanders, A.-M., Richard, G., Kolskår, K., Ulrichsen, K. M., Kaufmann, T., Alnæs, D., Beck, D., Dørum, E. S., de Lange, A.-M. G., Egil Nordvik, J., & Westlye, L. T. (2021). Linking objective measures of physical activity and capability with brain structure in healthy community dwelling older adults. *NeuroImage: Clinical*, *31*, 102767. https://doi.org/10.1016/j.nicl.2021.102767

Schindler, L. S., Subramaniapillai, S., Barth, C., van der Meer, D., Pedersen, M. L., Kaufmann, T., Maximov, I. I., Linge, J., Leinhard, O. D., Beck, D., Gurholt, T. P., Voldsbekk, I., Suri, S., Ebmeier, K. P., Draganski, B., Andreassen, O. A., Westlye, L. T., & de Lange, A.-M. G. (2022). Associations between abdominal adipose tissue, reproductive span, and brain characteristics in post-menopausal women. *NeuroImage: Clinical*, *36*, 103239. https://doi.org/10.1016/j.nicl.2022.103239

Sebastiani, P., Thyagarajan, B., Sun, F., Schupf, N., Newman, A. B., Montano, M., & Perls, T. T. (2017). Biomarker signatures of aging. *Aging Cell*, *16*(2), 329–338. https://doi.org/10.1111/acel.12557

Smith, S. M., Jenkinson, M., Johansen-Berg, H., Rueckert, D., Nichols, T. E., Mackay, C. E., Watkins, K. E., Ciccarelli, O., Cader, M. Z., Matthews, P. M., & Behrens, T. E. J. (2006). Tract-based spatial statistics: Voxelwise analysis of multi-subject diffusion data. *NeuroImage*, *31*(4), 1487–1505. https://doi.org/10.1016/j.neuroimage.2006.02.024

Spauwen, P. J. J., Murphy, R. A., Jónsson, P. V., Sigurdsson, S., Garcia, M. E., Eiriksdottir, G., van Boxtel, M. P. J., Lopez, O. L., Gudnason, V., Harris, T. B., & Launer, L. J. (2017). Associations of fat and muscle tissue with cognitive status in older adults: The

AGES-Reykjavik Study. *Age and Ageing*, *46*(2), 250–257. https://doi.org/10.1093/ageing/afw219

Subramaniapillai, S., Suri, S., Barth, C., Maximov, I. I., Voldsbekk, I., van der Meer, D., Gurholt, T. P., Beck, D., Draganski, B., Andreassen, O. A., Ebmeier, K. P., Westlye, L. T., & de Lange, A.-M. G. (2022). Sex- and age-specific associations between cardiometabolic risk and white matter brain age in the UK Biobank cohort. *Human Brain Mapping*, *n/a*(n/a). https://doi.org/10.1002/hbm.25882

Szymczak, J., Milewicz, A., Thijssen, J. H. H., Blankenstein, M. A., & Daroszewski, J. (1998). Concentration of Sex Steroids in Adipose Tissue after Menopause. *Steroids*, *63*(5), 319–321. https://doi.org/10.1016/S0039-128X(98)00019-1

Tian, Y. E., Cropley, V., Maier, A. B., Lautenschlager, N. T., Breakspear, M., & Zalesky, A. (2023). Heterogeneous aging across multiple organ systems and prediction of chronic disease and mortality. *Nature Medicine*, 1–11. https://doi.org/10.1038/s41591-023-02296-6

Tyrrell, J., Zheng, J., Beaumont, R., Hinton, K., Richardson, T. G., Wood, A. R., Davey Smith, G., Frayling, T. M., & Tilling, K. (2021). Genetic predictors of participation in optional components of UK Biobank. *Nature Communications*, *12*(1), Article 1. https://doi.org/10.1038/s41467-021-21073-y

Voldsbekk, I., Barth, C., Maximov, I. I., Kaufmann, T., Beck, D., Richard, G., Moberget, T., Westlye, L. T., & de Lange, A.-M. G. (2021). A history of previous childbirths is linked to women's white matter brain age in midlife and older age. *Human Brain Mapping*, *42*(13), 4372–4386. https://doi.org/10.1002/hbm.25553

Wagenmakers, E.-J., Lodewyckx, T., Kuriyal, H., & Grasman, R. (2010). Bayesian hypothesis testing for psychologists: A tutorial on the Savage–Dickey method.

Cognitive Psychology, *60*(3), 158–189. https://doi.org/10.1016/j.cogpsych.2009.12.001

West, J., Romu, T., Thorell, S., Lindblom, H., Berin, E., Holm, A.-C. S., Åstrand, L. L., Karlsson, A., Borga, M., Hammar, M., & Leinhard, O. D. (2018). Precision of MRI-based body composition measurements of postmenopausal women. *PloS One*, *13*(2), e0192495. https://doi.org/10.1371/journal.pone.0192495

Wong, M. W., Braidy, N., Poljak, A., Pickford, R., Thambisetty, M., & Sachdev, P. S. (2017). Dysregulation of lipids in Alzheimer's disease and their role as potential biomarkers. *Alzheimer's & Dementia*, *13*(7), 810–827. https://doi.org/10.1016/j.jalz.2017.01.008